Radiological Physics and Technology
https://doi.org/10.1007/s12194-019-00546-2

Transbronchial biopsy of peripheral lung lesions using fluoroscopic guidance combined with an enhanced ray-summation display

Shogo Suzuki[1,2] · Katsuhiro Ichikawa[3] · Yasuhisa Kouno[1] · Naoya Takeda[4] · Yoshihiro Suzuki[4] · Ayumi Suzuki[5]

Received: 11 December 2018 / Revised: 13 November 2019 / Accepted: 14 November 2019

Abstract
The aim of this study was to investigate the effectiveness of guidance assistance during transbronchial biopsy (TBB) to achieve an appropriate pathway to small and peripheral pulmonary lesions (PPLs) using a combination of fluoroscopy and specialized ray-summation (Ray-sum$_{TBB}$) images, which were processed from preprocedural lung computed tomography (CT) images. To improve the visibility of the correct pathway to the PPLs, three-dimensional spatial resolution enhancement and CT number conversion processes were applied to the original CT images. The Ray-sum$_{TBB}$ images reconstructed from the processed CT images were used as additional guides. We compared the rates of successful tumor localization and biopsy (arrival rate) between the trial (with Ray-sum$_{TBB}$) and control (without Ray-sum$_{TBB}$) groups. The fluoroscopy and examination times were also compared. The arrival rate of the trial group (73.1%) was significantly better than that of the control group (42.3%) ($p = 0.048$). The fluoroscopy and examination times did not differ significantly between the trial and control groups. No complications were identified in the trial group. Our results suggest that Ray-sum$_{TBB}$ improves the diagnostic accuracy of TBB.

Keywords Transbronchial biopsy · Ray-summation · Frequency processing · Peripheral pulmonary lesion · Ground-glass opacity · Endobronchial ultrasound

1 Introduction

Flexible bronchoscopy is generally accepted as the gold standard method for assessing lung nodules. The minimally invasive transbronchial biopsy (TBB) assists in diagnosing lung diseases. Previous studies have reported that the diagnostic accuracy of TBB for peripheral pulmonary lesions (PPLs) exceeds 80.0% [1, 2]. However, according to the American College of Chest Physicians Lung Cancer Guidelines (2nd edition) [2], the diagnostic yield for lesions < 20 mm in diameter is as low as 34.0% [3]. However, PPLs that are > 8 mm are more likely to be malignant [4]. Thus, more accurate methods for diagnosing PPLs that are < 20 mm in diameter are required.

The diagnostic yield of TBB for PPLs depends on several factors, including the selected sampling method, lesion size, lesion location, and physician's skill [5-9]. Although computed tomography (CT)-guided TBB is an effective method for diagnosing PPLs [10, 11], it requires exposure to excess doses of radiation from repeated CT scanning [10]. To further improve the diagnostic yield, CT-guided TBB with virtual bronchoscopy navigation (VBN) is often performed [12-15]. Other novel hardware- and software-guided TBB techniques for improving the diagnostic yield of TBB have also been introduced and applied in clinical practice over the past decade [16-20]. Specifically, the bronchoscopic transparenchymal nodule access [16, 17], a method of pathway

✉ Shogo Suzuki
shogo.suzuki@toyota-kai.or.jp

1 Department of Radiological Technology, Kariya Toyota General Hospital, 5-15 Sumiyoshi-cho, Kariya 448-8505, Aichi, Japan

2 Graduate School of Medical Science, Kanazawa University, 5-11-80 Kodatsuno, Kanazawa 920-0942, Ishikawa, Japan

3 Institute of Medical, Pharmaceutical and Health Sciences, Kanazawa University, 5-11-80 Kodatsuno, Kanazawa 920-0942, Ishikawa, Japan

4 Department of Respiratory and Allergy Medicine, Kariya Toyota General Hospital, 5-15 Sumiyoshi-cho, Kariya 448-8505, Aichi, Japan

5 Department of Thoracic Surgery, Kariya Toyota General Hospital, 5-15 Sumiyoshi-cho, Kariya 448-8505, Aichi, Japan

Published online: 19 November 2019

planning using fluoroscopic guidance could effectively be used in performing procedures.

Fluoroscopic guidance is widely used during TBB; however, it is associated with some essential disadvantages. First, the guidance images are two-dimensional (2D) projections, which make it difficult to understand the three-dimensional (3D) anatomical relationships among the projected objects. Second, the contrast resolution of fluoroscopic guidance images is often insufficient, and sometimes suboptimal, specifically when low-radiation doses are used. Certainly, several PPLs that feature ground-glass opacities (GGOs) and low attenuation are not visible on fluoroscopic images [21, 22]. Yoshikawa et al. [23] even reported that adding fluoroscopy to TBB for PPLs that are < 20 mm has no diagnostic advantage. Although these disadvantages are known, fluoroscopic guidance remains popular, because most hospitals have fluoroscopic examination room(s) and it is easy to perform. The value of fluoroscopy in TBB remains to be clarified.

In this study, we propose a novel image guidance method for TBB of PPLs using ray-summation (Ray-sum$_{TBB}$) images, which are reconstructed from routine preprocedural CT images. This guidance technique is intended for use during TBB examinations with a thin bronchoscope, radial endobronchial ultrasound (EBUS) using a guide sheath [24], and fluoroscopic guidance (the routine TBB examination method in our hospital). The purpose of this study was to compare the rates of successful tumor localization and biopsy (arrival rate) between TBB in combination with Ray-sum$_{TBB}$ image guidance and TBB alone.

2 Materials and methods

2.1 Ray-summation images for transbronchial biopsy (TBB) assistance

The ray-summation technique used to generate Ray-sum$_{TBB}$ is an application consisting of 3D-CT images, typically implemented in commercially available 3D-CT workstations. The technique produces projection images, which mimic general radiographs, by projecting (adding) voxel data in a CT volume data, along each projection path (ray). The volume data are typically constructed with consecutive thin-slice CT images. In general, the ray-summation images can be manipulated using a computer mouse, enabling the observer to freely change the projection angle. Thus, the observer can view the mimicked radiograph from any angle as if the observer changes the patient's posture during fluoroscopy. Our proposed method combines this ray-summation image display with fluoroscopy to improve the guidance during TBB of PPLs. We initially tested normal ray-summation images for TBB assistance. However, the bronchoscopists in our TBB team declined the use of the normal ray-summation images, because the images provided only a slight contrast enhancement and the image resolution was insufficient.

We applied several image processing techniques to the CT image dataset to improve the visibility of the endoscopic pathway (tracheobronchial tree to the lesion) and tumor within the Ray-sum$_{TBB}$ images. The outline flow of the processes is presented in Fig. 1. Ray-summation images typically have insufficient spatial resolution, because the matrix size of the original CT images is limited to 512 × 512. This is significantly inferior to those of digital fluoroscopic images having at least 1024 × 1024 matrix size; hence, we first applied 3D spatial resolution enhancement [25, 26] to the CT image set using in-house software developed by MATLAB version R2016a (MathWorks Inc., Novi, MI, USA). First, the CT image data (i.e., the 3D volume data) were transformed to 3D Fourier domain data using a 3D Fourier transformation. Following this, the 2D frequency processing factor for each slice (x–y) plane, as shown in Fig. 2a, was multiplied to each plane. Subsequently, a one-dimensional frequency processing factor for the longitudinal (z) direction, as shown in Fig. 2b, was multiplied to each z-directional profile at all x, y positions. Finally, the processed (enhanced)

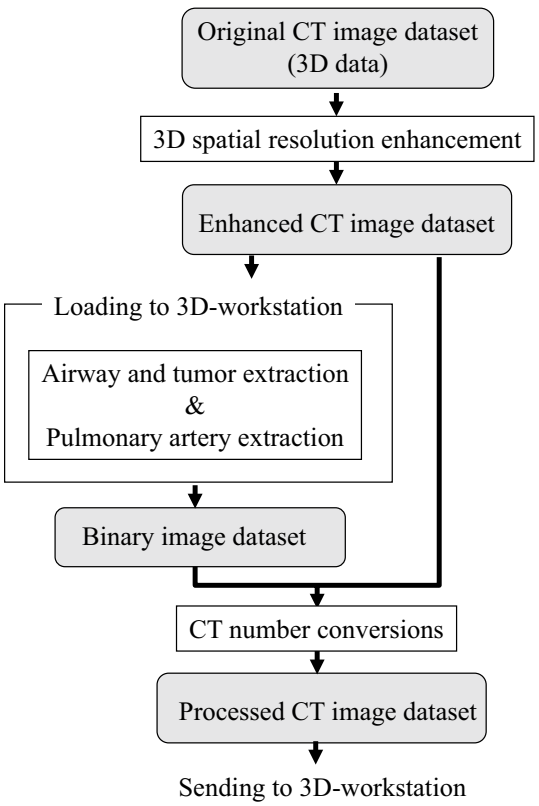

Fig. 1 Outline process flow for enhancing the computed tomography image dataset used for reconstructing ray-summation images. The reconstructed ray-summation images were used as additional guidance images in transbronchial biopsy examination

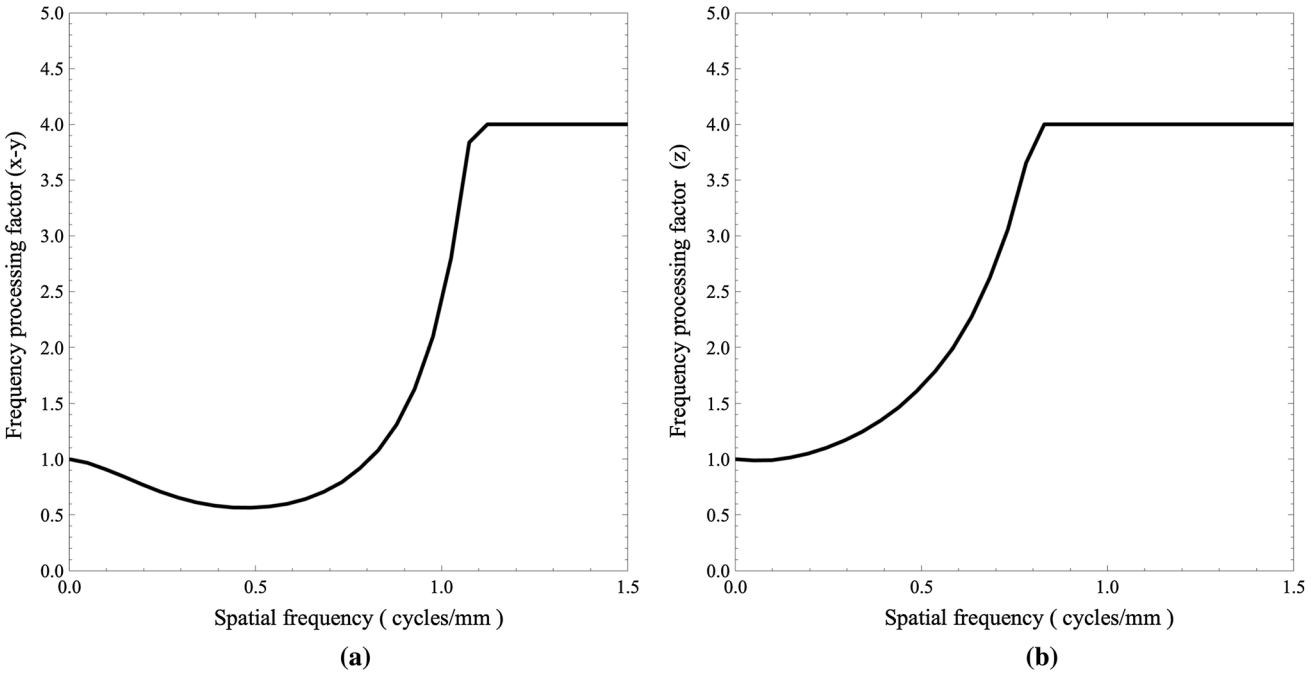

Fig. 2 Spatial frequency processing factors were calculated from the ratio of modulation transfer factor obtained from the flat panel detector of fluoroscopy system and computed tomography. Spatial frequency processing factors for the **a** *x*–*y* plane and **b** *z* direction that were applied to the original computed tomography image dataset for improving the spatial resolution of ray-summation images to a level that was similar to that of fluoroscopic images

3D volume data were obtained using an inverse 3D Fourier transformation.

Following the above-mentioned spatial resolution enhancement, the data were once loaded to the 3D-CT workstation (Zio Station2; Ziosoft, Tokyo, Japan) to extract the airway and tumor. The pathway was identified using several operations in the 3D-CT workstation, with a threshold of -940 Hounsfield units (HU). The tumor was identified using a 3D region of interest tool with appropriate thresholding depending on the CT number of tumor. Onodera et al. [27] previously demonstrated the advantages of using the pulmonary artery bundled with the bronchus to predict a more peripheral route. Therefore, we identified the pulmonary artery, using a threshold of around -60 HU, when peripheral bronchi were not visible on CT images. The identified regions were exported as 2D binary images with the same slice (image) number and matrix size of the original CT images. Subsequently, we applied CT number conversion processing to the CT image set using in-house software with MATLAB, referring to the 2D binary images. The CT number of the pathway was converted to + 6000 HU to simulate the bronchography using a contrast medium. The CT numbers of the tumor and pulmonary artery were converted to + 4000 HU and + 5000 HU, respectively. These HU conversion processes enable to observe three objects (pathway, tumor, and pulmonary artery) with different contrast. The processed CT image set was again loaded into the 3D-CT workstation, and the Ray-sum$_{TBB}$ image was visualized on the 3D-CT workstation display. Figure 3 shows the examples of a normal ray-sum image, Ray-sum$_{TBB}$ image, and digital radiograph for the same patient. The Ray-sum$_{TBB}$ image had markedly improved spatial resolution and resembled the digital radiographic depiction. The images in this study were obtained after the institutional ethics review board approved this study. Figure 4 shows Ray-sum$_{TBB}$ images with enhanced airways, enhanced pulmonary arteries, and enhanced airways and pulmonary arteries for comparison. Figure 5 shows the display layout during the TBB examination with Ray-sum$_{TBB}$. The fluoroscopic and Ray-sum$_{TBB}$ images are displayed side by side throughout the procedure. During TBB, the assistant radiologist manipulated the computer mouse of the 3D-CT workstation to select the optimal viewing angles and magnifications, according to the fluoroscopic images being displayed during the TBB examination. The automatic image matching and registration processes were not included in our technique.

The motivation for our approach is attributed to the clinical demand of the bronchoscopists in our TBB team to observe the fluoroscopy image more clearly and to identify thinner bronchia, tumors, and, if possible, arteries around the bronchus. It has been well known that the fluoroscopy-like images are generated by the ray-summation process using a 3D-CT image dataset; however, the bronchus is not clearly visualized by normal ray-summation image as is; moreover,

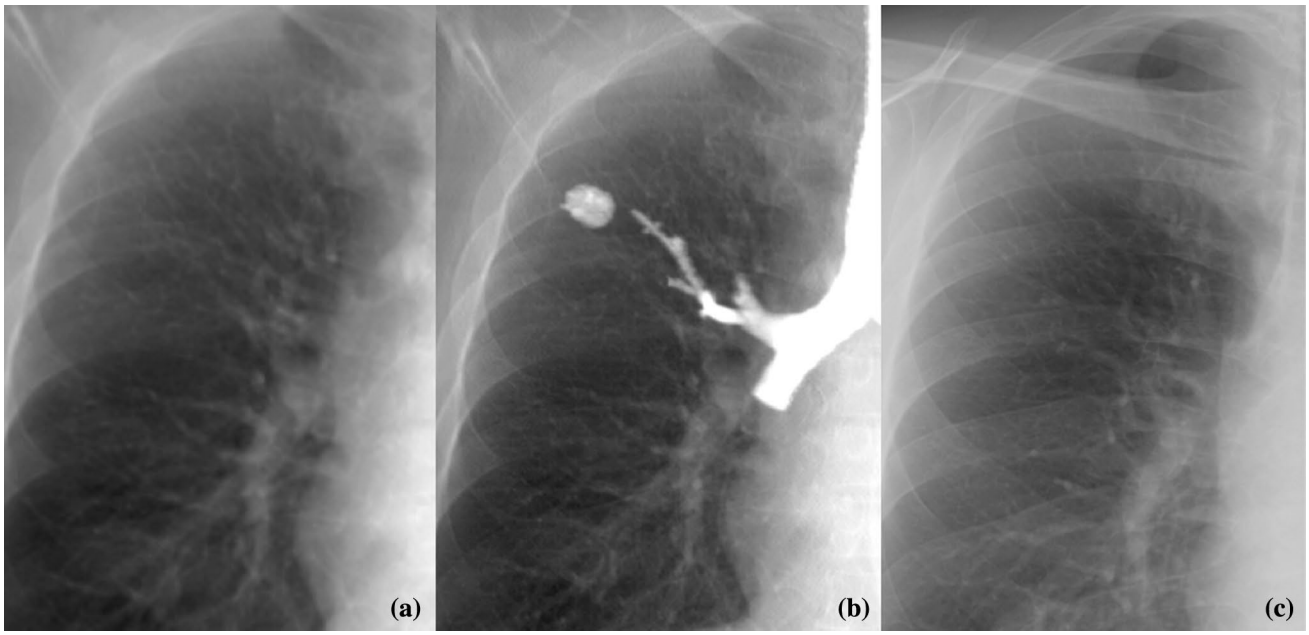

Fig. 3 Examples of **a** normal ray-summation **b** ray-summation for transbronchial biopsy (Ray-sum$_{TBB}$), and **c** digital radiography images acquired from a single patient. The spatial resolution was markedly improved in the Ray-sum$_{TBB}$ image, approaching that of the digital radiography image

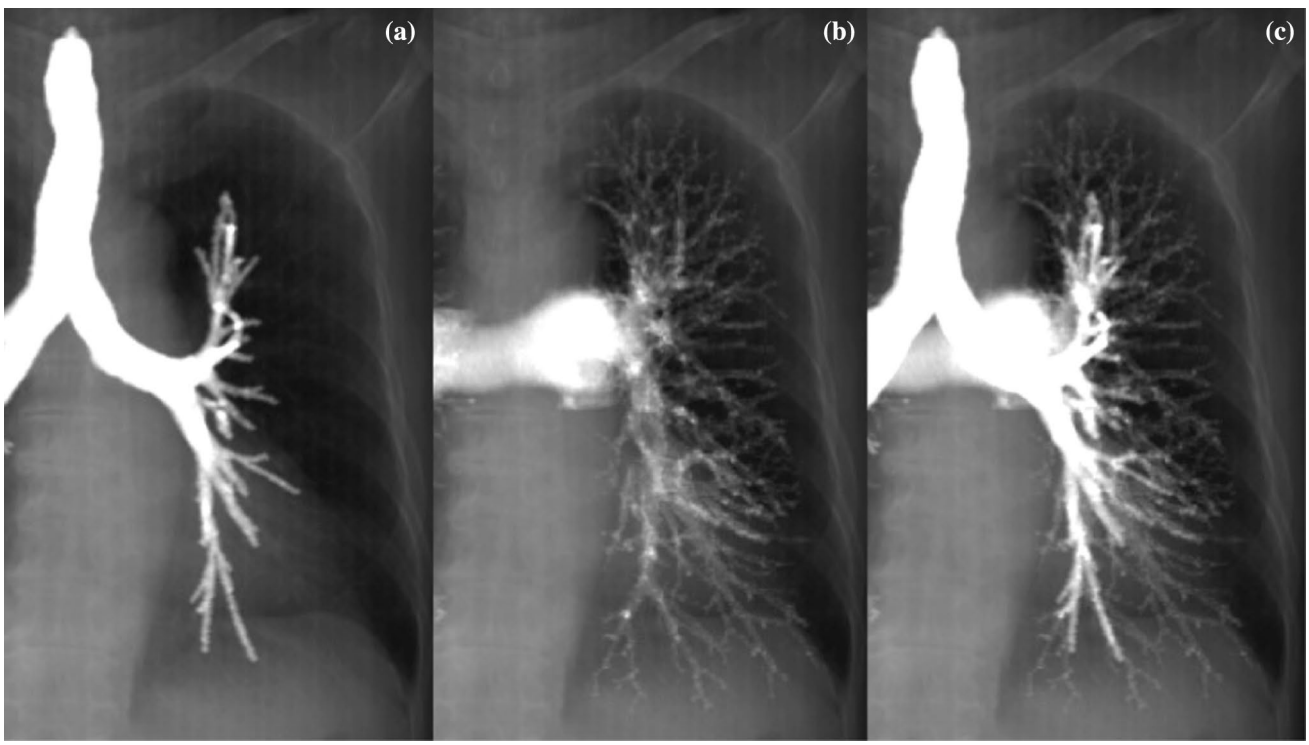

Fig. 4 Comparison of ray-summation images for transbronchial biopsy with **a** enhanced airways **b** enhanced pulmonary arteries, and **c** enhanced airways and pulmonary arteries

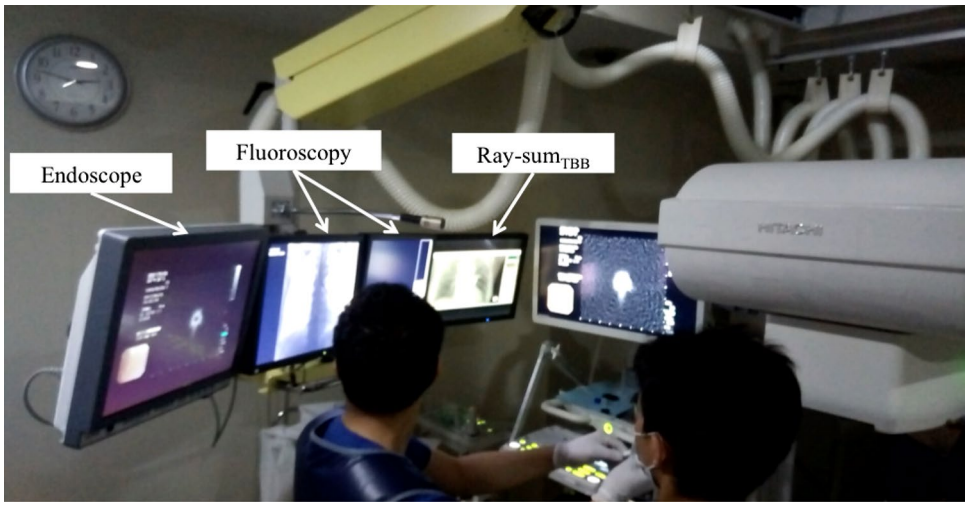

Fig. 5 Display layout during the transbronchial biopsy examination with ray-summation (Ray-sum$_{TBB}$) assistance

Table 1 Baseline characteristics of patients in the control (without Ray-sum$_{TBB}$) and trial (with Ray-sum$_{TBB}$) groups

Characteristic	Control group	Trial group	*p* value
Period	2016.1–2016.6	2016.7–2016.12	
Age (years)	68.6 ± 10.6	66.3 ± 14.2	0.072
Males:females	15:11	19:7	0.382
Tumor size (mm)	16.3 ± 2.4	15.3 ± 2.9	0.174
Existing GGO	1	4	0.350
Not visible in fluoroscopy	7	15	0.048*

*Statistically significant difference $p < 0.05$

identification of small tumors and arteries around the bronchus is often difficult. Thus, the spatial resolution enhancement and CT number conversions, which were specialized for TBB, were required items.

2.2 Patient population

This study was approved by our institutional ethics review board, and all patients provided informed consent for inclusion in the study. We enrolled 26 consecutive patients between July and December 2016 in the TBB examination with the Ray-sum$_{TBB}$ (trial) group. For the control group, we retrospectively reviewed the cases of 26 patients in whom TBB was performed without Ray-sum$_{TBB}$ between January and June 2016. Eligible patients had PPLs with diameters < 20 mm positioned in the peripheral bronchus. The PPLs were not directly visible through the endoscope. The baseline clinical characteristics of the population are presented in Table 1. No significant between-group differences in age, sex, or lesion size were identified. One patient in the control group and four patients in the trial group exhibited GGOs. Seven patients in the control group and 15 patients in the trial group had tumors that were not visible on fluoroscopic images.

2.3 Computed tomography scanning

Preprocedural CT examinations were performed for all patients within 1 week prior to each TBB examination using a 64-slice multi-detector row CT scanner (Aquilion CXL; Canon Medical, Otawara, Japan). The scanning parameters were as follows: 120 kVp; detector configuration, 64 × 0.5 mm; pitch factor, 0.54; and 0.5 s/rotation. Automatic tube current modulation (Real EC; Canon medical) was used with a prescribed noise index of 10 to adjust the radiation doses. Reconstruction parameters included a slice thickness of 0.5 mm, increments of 0.25 mm, and a reconstruction kernel of FC81 for the lung. The resultant volume CT dose index values ranged from 14.1 to 23.6 mGy. The above-mentioned scan was routine-based; thus, we did not perform any additional scans for obtaining Ray-sum$_{TBB}$. The size of each PPL was measured along the minimal and maximal diameters by the three radiologists with 35, 28, and 13 years of experience and recorded in the patient's medical record.

2.4 TBB examination

Each patient was premedicated with 15 mg of pentazocine hydrochloride and 0.5 mg of atropine sulfate. Local anesthesia of the upper respiratory tract was achieved with 4% lidocaine, in line with the standard of care for TBB. Examinations were performed using an ultrathin bronchoscope with an external diameter of 2.8 mm (BF-P260F; Olympus, Tokyo, Japan) in combination with a miniature ultrasound probe (20 MHz, mechanical radial type, UM-S20-20R; Olympus) and a guide sheath kit (SG-201C; Olympus). The probe was connected to an EBUS system

(EVIS LUCERA; EU-ME2; Olympus). We used 1.0-mm-diameter biopsy forceps (FD-44-D-1; Olympus). If needed, a double-hinged curette (CC-6DR-1; Olympus) was used to direct the guide sheath. We used the CUREVISTA fluoroscopy system (Hitachi, Ltd., Tokyo, Japan). All examinations were performed by two pulmonologists with 17 and 10 years of experience, respectively. The other staff consisted of one nurse and one radiological technologist. Complications such as hemoptysis and pneumothorax were recorded. Fluoroscopy times and examination times were measured to evaluate the outcomes associated with the two guidance techniques. Fluoroscopy times were obtained from the fluoroscopy system, and examination times were obtained from the Solemio endoscopy system (Olympus) at the end of the procedure.

2.5 Evaluation and analysis

We evaluated the arrival rate, rather than the diagnostic yield, which is typically assessed in TBB studies, because this study aimed to evaluate the effectiveness of fluoroscopy combined with Ray-sum$_{TBB}$ for correctly guiding the forceps to the tumor; as such, the diagnostic yields of this study mean the same as the arrival rates. All patients suspected to have cancer were not pathologically confirmed.

We used Student's *t* tests to compare the average fluoroscopy and examination times as continuous variables and Fisher's exact test to compare the arrival rates as categorical variables. The statistical software Statistical Package for the Social Sciences (SPSS), version 24 for Windows (SPSS Inc., Chicago, IL, USA), was used for all statistical analyses. Differences were considered statistically significant at $p < 0.05$.

3 Results

Table 2 shows the resultant arrival rates, fluoroscopy times, and examination times for each of the two groups (trial and control). The arrival rate was significantly higher in the trial group than that of the control group ($p = 0.048$). Among patients whose tumors were not visible on fluoroscopic images, the trial group showed a slightly, but not significantly, higher arrival rate than did the control group. No significant between-group differences in the fluoroscopy times or examination times were identified. Detailed results are shown in Table 3 (control group) and 4 (trial group).

Table 2 Arrival rate, fluoroscopy time, and examination time in the control and trial groups

	Control group	Trial group	*p* value
Arrival rate (%)	42.3 (11/26)	73.1 (19/26)	0.048*
Arrival rate (%) (not visible in fluoroscopy)	28.6 (2/7)	60.0 (9/15)	0.361
Fluoroscopy time (min)	7.8 ± 3.1	8.9 ± 2.8	0.970
Examination time (min)	32.1 ± 10.1	27.1 ± 7.1	0.365

ns not significant

* Statistically significant difference $p < 0.05$

4 Discussion

During fluoroscopic guidance for TBB, spatial information is only provided in two dimensions, and there tends to be insufficient contrast resolution, specifically in the peripheral bronchi and for GGOs. These weaknesses frequently lead to uncertain and inadequate guidance. To improve the guidance during TBB, we introduced a method that employed Ray-sum$_{TBB}$ assistance. Using the Ray-sum$_{TBB}$ images, the bronchus, pathway, and tumor (and pulmonary artery in two patients) were clearly visible, enabling easy angulation according to the fluoroscopic images. No complaints related to the procedure were recorded by either pulmonologist. In one patient in whom pulmonary artery enhancement was observed (No. 45 in Table 4), the forceps reached the tumor because of guidance assistance, in combination with the pulmonary artery display. Even when the bronchoscope moved unexpectedly due to coughing or body movements, the bronchoscopist was able to identify a deviation by comparing between Ray-sum$_{TBB}$ of pathway and fluoroscopic image of the catheter head position. This enabled a smooth recovery following the disturbance and continued advancement of the forceps. Thus, adding Ray-sum$_{TBB}$ did not complicate the TBB procedure, and no significant fluoroscopy or examination time differences (extensions) were observed between TBB with and without Ray-sum$_{TBB,}$ although we expected that the Ray-sum$_{TBB}$ assistance shortens the fluoroscopy and examination times. As a result, no increase in radiation exposure to the patients and pulmonologists were caused by adding the assistance of Ray-sum$_{TBB}$.

Here, TBB with Ray-sum$_{TBB}$ was associated with a significantly better arrival rate, although the trial group included more patients in whom the PPLs were not visible on fluoroscopic images compared to the control group. Oki et al. [28] conducted a multicenter study that compared the diagnostic yields between patients who underwent EBUS, fluoroscopy, and VBN guidance with a 3.0-mm ultrathin bronchoscope or a 4.0-mm thin bronchoscope with a guide sheath. In that study, the diagnostic yields were 74% (median lesion size, 19.0) in the 3.0-mm ultrathin bronchoscope group and 59% (median lesion size, 19.4 mm) in the 4.0-mm thin bronchoscope with a guide sheath group [28]. Another study comparing patients who did and did not receive VBN assistance found diagnostic yields of 67.1% (median lesion size, 17.5 mm) in the VBN-assisted group and 59.9% (median lesion size, 17.0 mm) in the

Table 3 Detailed results for the control group

No	Age (years)	Sex	Tumor location	Average tumor size (mm)	Tumor property	Was PPL identified?	Diagnosis of EBUS	Diagnosis	Examination time (min)	Fluoroscopy time (min)	Applicable ray-sum
1	66	Female	LL[e]	13.0		Yes	–	–	0:21:54	0:07:02	NA[f]
2	68	Male	RU[a]	17.5		Yes	Arrived	Adenocarcinoma	0:37:32	0:09:28	NA
3	72	Female	RM[b]	16.2		Yes	Arrived	Adenocarcinoma	0:22:49	0:08:42	NA
4	70	Male	LL	19.2		No	–	–	0:23:30	0:03:27	NA
5	65	Female	LU[d]	18.2		Yes	–	–	0:28:48	0:07:41	NA
6	40	Male	RU	18.8		Yes	–	–	0:15:01	0:03:50	NA
7	72	Female	RM	18.9		Yes	–	–	0:27:55	0:05:06	NA
8	80	Male	LL	18.1		No	–	–	0:28:35	0:06:25	NA
9	68	Male	LU	15.1		Yes	–	–	0:22:40	0:09:13	NA
10	66	Female	LU	18.8		Yes	–	–	0:28:00	0:07:23	NA
11	54	Male	RU	19.5		Yes	Arrived	Small	0:25:38	0:09:47	NA
12	69	Male	LU	19.0		No	Arrived	No evidence of malignancy	0:30:53	0:07:14	NA
13	83	Male	RM	13.5		No	–	–	0:29:54	0:10:19	NA
14	81	Female	RL[c]	15.1		Yes	–	–	0:29:04	0:11:01	NA
15	82	Female	LL	15.2		No	–	–	0:29:36	0:13:47	NA
16	68	Male	RM	16.1		Yes			0:25:12	0:08:23	NA
17	63	Female	LU	19.7		Yes	Arrived	No evidence of malignancy	0:28:34	0:02:52	NA
18	77	Female	RM	15.9		Yes	Arrived	No evidence of malignancy	0:28:11	0:06:33	NA
19	67	Male	LU	15.5		Yes	Arrived	Adenocarcinoma	0:28:22	0:12:46	NA
20	56	Female	RM	16.9		Yes	Arrived	No evidence of malignancy	0:30:10	0:05:53	NA
21	72	Male	RU	12.0		Yes	Arrived	No evidence of malignancy	1:02:54	0:11:39	NA
22	68	Female	RU	13.0		No	Arrived	No evidence of malignancy	0:37:40	0:09:17	NA
23	78	Female	LU	12.9	GGO	No	–	–	0:25:09	0:05:37	NA
24	45	Male	RL	17.0		Yes	–	–	0:53:21	0:03:22	NA
25	80	Male	RL	17.5		Yes	Arrived	Squamous cell carcinoma	0:46:02	0:08:22	NA
26	73	Male	RU	12.4		Yes	–	–	1:07:50	0:05:30	NA

[a]Right upper lobe

[b]Right middle lobe

[c]Right lower lobe

[d]Left upper lobe

[e]Left lower lobe

[f]Not applicable

Table 4 Detailed results for the trial group

No.	Age (years)	Sex	Tumor location	Average tumor size (mm)	Tumor property	Was PPL identified?	Diagnosis of EBUS	Diagnosis	Examination time (min)	Fluoroscopy time (min)	Applicable ray-sum
27	56	Male	LL[e]	16.8	GGO	No	Arrived	No evidence of malignancy	0:34:40	0:12:53	Ray-sum$_B$[f]
28	47	Male	RL	19.3		No	–	–	0:21:59	0:10:23	Ray-sum$_B$
29	56	Male	RU[a]	14.8		Yes	Arrived	Adenocarcinoma	0:23:28	0:05:07	Ray-sum$_B$
30	77	Male	LU[d]	11.8		Yes	Arrived	Squamous cell carcinoma	0:31:18	0:07:26	Ray-sum$_B$
31	61	Male	RM[b]	16.8		Yes	Arrived	No evidence of malignancy	0:23:58	0:07:02	Ray-sum$_B$
32	67	Female	LL	17.1		No	Arrived	Adenocarcinoma	0:26:54	0:03:49	Ray-sum$_B$
33	39	Male	RL[c]	14.1		Yes	Arrived	Adenocarcinoma	0:30:26	0:11:34	Ray-sum$_B$
34	73	Male	RL	12.0		No	Arrived	Adenocarcinoma	0:18:29	0:03:31	Ray-sum$_B$
35	47	Female	RL	12.1	GGO	No	–	–	0:17:42	0:09:36	Ray-sum$_{B+PA}$[g]
36	57	Female	RL	18.6		Yes	Arrived	No evidence of malignancy	0:15:51	0:05:26	Ray-sum$_B$
37	75	Male	RU	9.6		No	Arrived	Adenocarcinoma	0:29:36	0:08:48	Ray-sum$_B$
38	74	Male	RM	14.5		No	–	–	0:29:45	0:10:01	Ray-sum$_B$
39	83	Male	RM	19.5		No	Arrived	No evidence of malignancy	0:27:48	0:11:22	Ray-sum$_B$
40	75	Male	LU	17.5		Yes	Arrived	Small	0:23:43	0:08:15	Ray-sum$_B$
41	59	Male	LL	12.1		Yes	Arrived	No evidence of malignancy	0:25:18	0:07:43	Ray-sum$_B$
42	73	Female	RM	17.5		No	–	–	0:17:17	0:04:53	Ray-sum$_B$
43	85	Female	RM	18.7	GGO	No	Arrived	No evidence of malignancy	1:07:50	0:09:05	Ray-sum$_B$
44	30	Male	RL	19.3		No	Arrived	Small	0:29:13	0:10:55	Ray-sum$_B$
45	77	Female	RM	10.6		No	Arrived	Adenocarcinoma	0:21:19	0:05:51	Ray-sum$_{B+PA}$
46	79	Male	LL	17.5		Yes	–	–	0:22:39	0:12:13	Ray-sum$_B$
47	62	Male	RL	16.5		Yes	Arrived	Squamous cell carcinoma	0:28:28	0:10:09	Ray-sum$_B$
48	81	Male	RU	15.5		Yes	Arrived	Adenocarcinoma	0:42:16	0:13:20	Ray-sum$_B$
49	68	Female	RU	13.5		Yes	Arrived	Adenocarcinoma	0:19:24	0:11:21	Ray-sum$_B$
50	81	Male	RU	12.4		No	Arrived	Adenocarcinoma	0:23:05	0:09:52	Ray-sum$_B$
51	74	Male	RL	17.5		No	–	–	0:31:44	0:12:08	Ray-sum$_B$
52	67	Male	RU	13.7	GGO	No	–	–	0:19:34	0:09:23	Ray-sum$_B$

[a]Right upper lobe

[b]Right middle lobe

[c]Right lower lobe

[d]Left upper lobe

[e]Left lower lobe

[f]Ray-summation image with enhanced bronchus

[g]Ray-summation image with enhanced bronchus and pulmonary artery

non-VBN-assisted group [29]. The results of the present study, which examined the arrival rate rather than the diagnostic yield, were comparable to that of the previous studies. It should be noted that while VBN assistance provides endoscopic-like 3D images for guidance assistance, our technique provides fluoroscopic-like projection images. Collectively, our results demonstrated that fluoroscopic-like projection images also provide effective guidance assistance during TBB.

The present study had several limitations. First, Ray-sum$_{TBB}$ only expresses the patient's status during breath holding. When a patient cannot hold his or her breath during TBB, differences between the fluoroscopy and Ray-sum$_{TBB}$ images may be induced by respiration, specifically near the diaphragm [30]. Second, our sample size was small (26 patients in each group), the tumor locations were not similar between the control and trial groups, and the study design was nonrandomized. Therefore, additional randomized trials of Ray-sum$_{TBB}$ are required to confirm our findings. Moreover, the assistance method using Ray-sumTBB should be improved, aiming to shorten the examination time and reduce the radiation dose. Nevertheless, following the conclusion of this study, the bronchoscopists at our hospital have continued to use our technique employing Ray-sum$_{TBB}$ assistance; thus, we believe that this technique may help improve the diagnostic yield of TBB for PPLs.

5 Conclusion

In the present study, we proposed and tested the utility of Ray-sum$_{TBB}$ image-assisted guidance for locating PPLs during TBB examinations under fluoroscopy. Our results demonstrated that this new technique improved the arrival rate at PPLs, without increasing the fluoroscopy and examination times. Ray-sum$_{TBB}$ opened new possibilities for a strong navigation tool, and the current study is considered significant in establishing the diagnosis of TBB.

Compliance with ethical standards

Conflict of interest None of the authors has any conflicts of interest to disclose.

Ethical approval All procedures performed in studies involving human participants were in accordance with the ethical standards of the Institutional Review Board (IRB) and with the 1964 Helsinki Declaration and its later amendments or comparable ethical standards. This article does not contain any studies with animals.

Informed consent Informed consent was obtained from all study participants.

References

1. Eberhardt R, Anantham D, Ernst A, Feller-Kopman D, Herth F. Multimodality bronchoscopic diagnosis of peripheral lung lesions: a randomized controlled trial. Am J Respir Crit Care Med. 2007;176:36–41.
2. Wang Memoli JS, Nietert PJ, Silvestri GA. Meta-analysis of guided bronchoscopy for the evaluation of the pulmonary nodule. Chest. 2012;142:385–93.
3. Rivera MP, Mehta AC. Initial diagnosis of lung cancer: ACCP evidence-based clinical practice guidelines. Chest. 2007;132:131S–48S.
4. Gould MK, Donington J, Lynch WR, Mazzone PJ, Midthun DE, Naidich DP, Wiener RS. Evaluation of individuals with pulmonary nodules: when is it lung cancer? Diagnosis and management of lung cancer, 3rd ed: American College of Chest Physicians evidence-based clinical practice guidelines. Chest. 2013;143:e93S–e120S.
5. Herth FJ, Eberhardt R, Becker HD, Ernst A. Endobronchial ultrasound-guided transbronchial lung biopsy in fluoroscopically invisible solitary pulmonary nodules: a prospective trial. Chest. 2006;129:147–50.
6. Eberhardt R, Anantham D, Herth F, Feller-Kopman D, Ernst A. Electromagnetic navigation diagnostic bronchoscopy in peripheral lung lesions. Chest. 2007;131:1800–5.
7. Kikuchi E, Yamazaki K, Sukoh N, Kikuchi J, Asahina H, Imura M, Nishimura M. Endobronchial ultrasonography with guide-sheath for peripheral pulmonary lesions. Eur Respir J. 2004;24:533–7.
8. Yamada N, Yamazaki K, Kurimoto N, Asahina H, Kikuchi E, Shinagawa N, Oizumi S, Nishimura M. Factors related to diagnostic yield of transbronchial biopsy using endobronchial ultrasonography with a guide sheath in small peripheral pulmonary lesions. Chest. 2007;132:603–8.
9. Ong PG, Debiane LG, Casal RF. Recent advances in diagnostic bronchoscopy. J Thorac Dis. 2016;8:3808–17.
10. Endo M, Kotani Y, Satouchi M, Takada Y, Sakamoto T, Tsubota N, Furukawa H. CT fluoroscopy-guided bronchoscopic dye marking for resection of small peripheral pulmonary nodules. Chest. 2004;125:1747–52.
11. Ost D, Shah R, Anasco E, Lusardi L, Doyle J, Austin C, Fein A. A randomized trial of CT fluoroscopic-guided bronchoscopy vs conventional bronchoscopy in patients with suspected lung cancer. Chest. 2008;134:507–13.
12. Asahina H, Yamazaki K, Onodera Y, Kikuchi E, Shinagawa N, Asano F, Nishimura M. Transbronchial biopsy using endobronchial ultrasonography with a guide sheath and virtual bronchoscopic navigation. Chest. 2005;128:1761–5.
13. Asano F, Matsuno Y, Shinagawa N, Yamazaki K, Suzuki T, Ishida T, Moriya H. A virtual bronchoscopic navigation system for pulmonary peripheral lesions. Chest. 2006;130:559–66.
14. Ishida T, Asano F, Yamazaki K, Shinagawa N, Oizumi S, Moriya H, Nunakata M, Nishimura M. Virtual bronchoscopic navigation combined with endobronchial ultrasound to diagnose small peripheral pulmonary lesions: a randomised trial. Thorax. 2011;66:1072–7.
15. Merritt SA, Gibbs JD, Yu KC, Patel V, Rai L, Cornish DC, Bascom R, Higgins WE. Image-guided bronchoscopy for peripheral lung lesions: a phantom study. Chest. 2008;134:1017–26.
16. Sterman DH, Keast T, Rai L, Gibbs J, Wibowo H, Draper J, Herth FJ, Silvestri GA. High yield of bronchoscopic transparenchymal nodule access real-time image-guided sampling in a novel model of small pulmonary nodules in canines. Chest. 2015;147:700–7.
17. Silvestri GA, Herth FJ, Keast T, Rai L, Gibbs J, Wibowo H, Sterman DH. Feasibility and safety of bronchoscopic

transparenchymal nodule access in canines: a new real-time image-guided approach to lung lesions. Chest. 2014;145:833–8.
18. Schwarz Y, Greif J, Becker HD, Ernst A, Mehta A. Real-time electromagnetic navigation bronchoscopy to peripheral lung lesions using overlaid CT images: the first human study. Chest. 2006;129:988–94.
19. Shinagawa N, Yamazaki K, Onodera Y, Miyasaka K, Kikuchi E, Dosaka-Akita H, Nishimura M. CT-guided transbronchial biopsy using an ultrathin bronchoscope with virtual bronchoscopic navigation. Chest. 2004;125:1138–43.
20. Edell E, Krier-Morrow D. Navigational bronchoscopy: overview of technology and practical considerations—new current procedural terminology codes effective 2010. Chest. 2010;137:450–4.
21. Ichikawa K, Kobayashi T, Sagawa M, Katagiri A, Uno Y, Nishioka R, Matsuyama J. A phantom study investigating the relationship between ground-glass opacity visibility and physical detectability index in low-dose chest computed tomography. J Appl Clin Med Phys. 2015;16:202–15.
22. Rose A. The sensitivity performance of the human eye on an absolute scale. J Opt Soc Am. 1948;38:196–208.
23. Yoshikawa M, Sukoh N, Yamazaki K, Kanazawa K, Fukumoto S, Harada M, Kikuchi E, Munakata M, Nishimura M, Isobe H. Diagnostic value of endobronchial ultrasonography with a guide sheath for peripheral pulmonary lesions without X-ray fluoroscopy. Chest. 2007;131:1788–93.
24. Kurimoto N, Miyazawa T, Okimasa S, Maeda A, Oiwa H, Miyazu Y, Murayama M. Endobronchial ultrasonography using a guide sheath increases the ability to diagnose peripheral pulmonary lesions endoscopically. Chest. 2004;126:959–65.
25. Ichikawa K, Kodera Y, Ohashi K, Sugiyama M, Miyachi T, Fujita H. Performance evaluation of computed tomography with equivalent resolution images. Nihon Hoshasen Gijutsu Gakkai Zasshi. 2006;62:522–8.
26. Suzuki S, Ichikawa K, Tamaki S. Image quality and clinical usefulness of ray-summation image reconstructed from CT data, compared with digital radiography. Nihon Hoshasen Gijutsu Gakkai Zasshi. 2017;73:372–81.
27. Onodera Y, Omatsu T, Takeuchi S, Shinagawa N, Yamazaki K, Nishioka T, Miyasaka K. Enhanced virtual bronchoscopy using the pulmonary artery: improvement in route mapping for ultraselective transbronchial lung biopsy. AJR Am J Roentgenol. 2004;183:1103–10.
28. Oki M, Saka H, Ando M, Asano F, Kurimoto N, Morita K, Kitagawa C, Kogure Y, Miyazawa T. Ultrathin bronchoscopy with multimodal devices for peripheral pulmonary lesions. A randomized trial. Am J Respir Crit Care Med. 2015;192:468–76.
29. Asano F, Shinagawa N, Ishida T, Shindoh J, Anzai M, Tsuzuku A, Oizumi S, Morita S. Virtual bronchoscopic navigation combined with ultrathin bronchoscopy. A randomized clinical trial. Am J Respir Crit Care Med. 2013;188:327–33.
30. Chen A, Pastis N, Furukawa B, Silvestri GA. The effect of respiratory motion on pulmonary nodule location during electromagnetic navigation bronchoscopy. Chest. 2015;147:1275–81.